1

Effect of Cavity Length and Operating Parameters on the Optical Performance of $Al_{0.08}In_{0.08}Ga_{0.84}N/ Al_{0.1}In_{0.01}Ga_{0.89}N$ MQW Laser Diodes

Alaa J. Ghazai*, H. Abu Hassan and Z. Hassan
Nano-Optoelectronics Research and Technology Laboratory,
School of Physics, Universiti Sains Malaysia,
Malaysia

1. Introduction

In this chapter, we discuss the effects of the cavity length of the active region in quaternary $Al_{0.08}In_{0.08}Ga_{0.84}N/Al_{0.1}In_{0.01}Ga_{0.89}N$ multiquantum-well (MQW) laser diodes (LD) on its performance. Semiconductor lasers emit coherent laser light with relatively small divergence and have long operating lifetimes because their very compact sizes can be easily integrated with a solid-state structure. They have very high efficiencies and need only a few milliwatts of power because they are cold light sources that operate at temperatures much lower than the equilibrium temperature of their emission spectra. The objective of the current study is to design the smallest possible semiconductor laser diode with good performance. The effects of various values of cavity length (ranging from 400–1200 nm) for $Al_{0.08}In_{0.08}Ga_{0.84}N/Al_{0.1}In_{0.01}Ga_{0.89}N$ MQW LD on laser parameters are investigated, including internal quantum efficiency η_i, internal loss α_i, and transparency current density J_0. High characteristic temperature and low transparency current of the $Al_{0.08}In_{0.08}Ga_{0.84}N/Al_{0.1}In_{0.01}Ga_{0.89}N$ MQW LD was obtained at a cavity length of 400 μm.

2. Overview

In the last decade of the 20th century, zinc selenide (ZnSe)-based quantum-well (QW) heterostructures in the blue-green spectrum were the first laser diodes (LD) investigated by Hasse et al. (1991) and(Haase 1991) (Jeon 1991)[1, 2]. However, rapid developments in III-nitride compounds by Nakamura et al. (1993) have brought LEDs based on these materials to technological capability and commerciality (Nakamura 1993)[3]. Violet InGaN QW LD under pulsed operation was demonstrated by Nakamura and Akasaki in 1996, and major improvements have since been achieved in its performance and device durability(Akasaki 1996; Nakamura 1996) [4, 5]. High-power LD (approximately 30 mW) was launched as a commercial product in September 2000(Nagahama 2000) [6]. Recently, aluminum indium

* Corresponding Author

gallium nitride (AlInGaN) alloys have been studied as the basis for next-generation optoelectronic applications, such as optical disk technology. Moreover, quaternary AlInGaN alloy has a wide band gap energy covering IR, visible, and UV regions, and permits an extra degree of freedom by allowing independent control of the band gap energy and lattice constant. The specific properties of III-nitride, such as its wide gap, high band offset, strong polarization fields, non-ideal alloy system, and so on, need to be identified for the design and optimum performance of LDs. Quaternary alloy has the issue of simultaneous incorporation of both In and Al, but offers the further quality of a "tunable" material, in terms of both the optical emission wavelength and lattice constant. Certainly, these issues are coupled with the control of the electrical properties of the p-n junction involved. Nagahama et al. (2001) studied both GaN and AlInGaN QW LD in the near-UV region, which has led to demonstrations of continuous-wave (CW)-edge-emitting lasers at room temperature near 370 nm(Nagahama 2001) [7].

Quaternary AlInGaN LDs with emission wavelengths less than 360 nm were also developed using Al and In content between 3% and 12% (Nagahama 2000; Nagahama S. 2001; Masui S. 2003; Michael K. 2003)[6, 8–10]. Wavelength "tunability" of the lasers was achieved for different Al and In compositions in the quaternary well, and, equally important, in the corresponding variations of the threshold current density J_{th}. In particular, an increase in J_{th} with increasing Al concentrations up to approximately 12 KA/cm^2 for x(Al) = 0.08 was noted. This increase was likely mainly the result of the quality of the quaternary $Al_xIn_yGa_{1-x-y}N$, in terms of both general morphology and defects (Nagahama S. 2001)[10]. A quaternary $Al_{0.03}In_{0.03}Ga_{0.94}N$ QW device under CW operation at room temperature, with a maximum output power reaching several milliwatts lasing at 366.4 nm, was also observed (Nagahama 2001)[6]. Shingo et al. reported $Al_{0.03}In_{0.03}Ga_{0.94}N$ UV LD under CW operation with emission wavelengths of 365 nm and a lifetime of 2000 h at an output power of 3 mW. They also achieved a short lasing wavelength of 354.7 nm under pulse current injection [8]. Michael et al. demonstrated room-temperature (RT) pulsed operation of AlInGaN MQW LD emission between 362.4 and 359.9 nm. Extending toward deep UV emission wavelength seemingly involves big challenges that become increasingly complicated with decreasing lasing wavelength [9]. Y. He et al. reported an optically pumped RT pulsed laser at 340 nm based on a separate confinement AlInGaN MQW heterostructure design [11]. The improvement of lasing characteristics, such as large optical gain and reduced threshold current of the GaN/AlInGaN QW laser using quaternary AlInGaN as a barrier, was reported by Seung et al. [12].

Recently, Michael et al. demonstrated the successful injection of AlInGaN ultravoliet laser on low dislocation density bulk AlN substrates using the MOCVD technique. The lasing wavelength was 368 nm under pulsed operation [13]. Thahab et al. reported ultraviolet quaternary AlInGaN MQW LDs using ISE TCAD software. For DQW, they simulated lasing wavelength of 355.8 nm under CW operation. However, the threshold current was high [14]. Overall, these initiatives encourage more development efforts on III-nitride materials as light emitters into deeper UV.

Several attempts have been made to improve the lasing characteristic and the reliability of the laser diodes in the last few years. The small active region in the laser diodes reduce the number of threading dislocation density (TDD) in the active region, which contributes to the fabrication of reliable laser diodes [15].

This chapter focuses on the simulation of edge emitting LD, whereas, in most other lasers, incorporation of an optical gain medium in a resonant optical cavity exists. The designs of both the gain medium and the resonant cavity are critical. The gain medium consists of a material that absorbs incident radiation over a wavelength range of interest. If it is pumped with either electrical or optical energy, the electrons within the material can be excited to higher, non-equilibrium energy levels. Therefore, the incident radiation may be amplified, rather than absorbed, by stimulating the de-excitation along with the generation of additional radiation. If the resulting gain is sufficient to overcome the losses of some resonant optical mode of the cavity, this mode is said to have reached its threshold, and coherent light will be emitted.

Resonant cavity provides the necessary positive feedback for the amplified radiation; lasing oscillation can be established nonstop above threshold pumping levels. As with any other oscillator, the output power saturates at a level equal to the input, minus any internal losses.

In this chapter, the effect of cavity length parameter on the optical performance of $Al_{0.08}In_{0.08}Ga_{0.84}N/Al_{0.1}In_{0.01}Ga_{0.89}N$ MQW LD is reported. Different important operating parameters are investigated, including internal quantum efficiency η_i, the internal loss α_i, characteristic temperature T_0, and transparency current density J_0 for our structure. For the lasers, these parameters are functions of the laser structure cavity dimension.

3. Oscillation condition of Fabry-Perot Laser

The simplest LD, Fabry-Perot LD, is realized by a pair of reflector mirrors facing each other, which are built together with the active material as resonator.

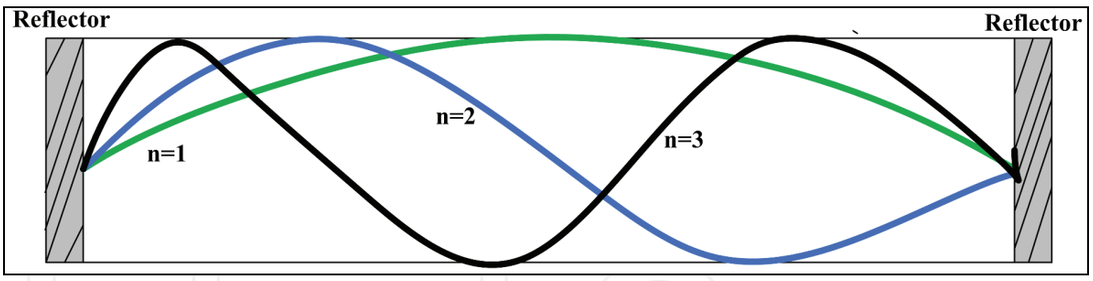

Fig. 1. Schematic description of a Fabry-Perot resonant cavity with reflecting facets on each end, the different modes supported within the cavity (n) exist in integer values.

For obtaining oscillation conditions, the plane optical waves traveling back and forth along the length of the laser are considered. These waves have optical frequencies of $\omega = 2\pi f$ with an associated propagation constant of $\beta = 2\pi\lambda_m$, where λ_m is the wavelength in the material. Such a wave, which starts from the left-hand reflector and travels to the right, is referred to as a forward wave, and has its phase and amplitude written in complex form:

$$E_f(z) = E_0 e^{(g-\alpha_i)z} e^{-j\beta z} e^{j\omega t} \tag{1}$$

The amplitude decays or grows with distance because the wave suffers scattering and other fixed losses α_i per unit length. However, it also experiences a material optical gain g per unit length caused by the stimulated recombination of electrons and holes. Consider that the

cavity length is L, the reflectivity of the right and left facets are R_1 and R_2, respectively, and there is no phase change on the reflection from the right facets at either end. The forward wave has a reflected fraction R_1 at the right facet (z = L). This fraction then travels back from right to left. According to Eq. (1), these reverse fields are described by

$$E_r(z) = \{ E_0 e^{(g-\alpha_i)L} e^{-j\beta L} \} e^{(g-\alpha_i)(L-z)} e^{-j\beta(L-z)} \tag{2}$$

where the time variation $e^{j\omega t}$ occurring in all terms is implicitly included.

The reverse wave travels back to the left facet ($z = 0$), and fraction R_2 is reflected to form the forward wave. For stable resonance, the amplitude and phase after this single whole round trip have to be identical with the phase and amplitude of the wave when it began:

$$E_0 = E_0 R_1 R_2 e^{(g-\alpha_i)2L} e^{-j2\beta L} \tag{3}$$

This gives the amplitude condition for stable oscillation:

$$R_1 R_2 e^{(g-\alpha_i)2L} = 1 \tag{4}$$

This could be also written as

$$g = \alpha_i + \frac{1}{2L} \ln\left(\frac{1}{R_1 R_2}\right) \tag{5}$$

where the logarithmic term can be considered as a distributed reflector loss α_m. Considering that only a fraction of the photons of the guided optical wave interacts with the active region, and considering the optical confinement factor Γ, Eq. (5) should be written as

$$\Gamma g = \alpha_i + \frac{1}{2L} \ln\left(\frac{1}{R_1 R_2}\right) = \alpha_i + \alpha_m \tag{6}$$

with,

$$\alpha_i = \alpha_0 (1 - \Gamma) + \alpha_g \Gamma \tag{7}$$

$$\alpha_m = \frac{1}{2L} \ln\left(\frac{1}{R_1 R_2}\right) \tag{8}$$

where α_i is the loss due to absorptions inside the guide α_g and outside α_0.

The differential quantum efficiency (DQE) depends on the internal quantum efficiency η_i and photon losses η_0:

$$\eta_d = \eta_i + \eta_0 \tag{9}$$

The photon loss value η_0 can be expressed as

$$\eta_0 = \frac{\alpha_m}{(\alpha_i + \alpha_m)} \tag{10}$$

where α_i is the internal loss and α_m is the optical mirror loss, which could be expressed as in Eq. (8). The DQE is dependent on the laser length L and the reflectivity of the mirror facets of laser, R_1 and R_2, as shown in the equation below:

$$\frac{1}{\eta_d} = \frac{1}{\eta_i} + \left(\frac{L\alpha_i}{\ln(1/R_1R_2)} + 1 \right) \tag{11}$$

The term $\eta_d^{-1}(L)$ is widely used to determine the internal quantum efficiency η_i and internal loss from (L-I) measurements with different laser lengths.

The natural logarithm of the threshold current density, ln (J_{th}), is plotted on the y-axis with temperatures on the x-axis; thus, the inverse of the slope of the linear fit to this set of data point is the characteristic temperature T_0:

$$T_0 = \frac{\Delta T}{\Delta \ln(J_{th})} \tag{12}$$

4. Laser structure and parameters used in numerical simulation

A two-dimensional (2D) ISE-TCAD laser simulation program is used in the simulation of the LDs, which is based on solving the Poisson and continuity equations of a 2D structure. The Poisson equation is given by [14, 16- 18]

$$\nabla.(\varepsilon \nabla \varphi) = q(n - p - N_D^+ + N_A^-) \tag{13}$$

where N_A is the acceptor doping density (cm^{-3}), N_D is the donor doping density (cm^{-3}), ε is the permittivity of them medium, □ is the potential energy, q is electron charge, and n and p are the number of electrons and holes, respectively. The electron and hole continuity equations are given by

$$\frac{\partial n}{\partial t} + \nabla.J_n = q(G_n - R_n) \tag{14}$$

$$\frac{\partial p}{\partial t} + \nabla.J_p = q(G_p - R_p) \tag{15}$$

where J_n and J_p are the current density of electron and hole, respectively; G_n and G_p are the electron generation rate and hole generation rate, respectively; and R_n, R_p are the electron recombination rate and hole recombination rate, respectively.

Physical models included are drift-diffusion transport with Fermi-Dirac statistic, surface recombination, Shockley-Read-Hall recombination, Auger recombination, and band gap narrowing at high doping levels. The UV LD structure was reported in our previous paper [18], which includes a 0.6 μm GaN contact layer, a cladding layer of n-$Al_{0.08}Ga_{0.92}N$/GaN modulation-doped strained superlattice (MD-SLS) that consists of eighty 2.5 nm pairs, and a

0.1 μm n-GaN wave-guiding layer. The active region consists of 3 nm $Al_{0.08}In_{0.08}Ga_{0.84}N$ MQW sandwiched between 6 nm $Al_{0.1}In_{0.01}Ga_{0.89}N$ barriers. Four other layers exists on top of the active region: a 0.02 μm p-$Al_{0.25}In_{0.08}Ga_{0.67}N$ blocking layer, a 0.1 μm p-GaN wave-guiding layer, and a cladding layer of p-$Al_{0.08}Ga_{0.92}N$/GaN MD-SLS consisting of eighty 2.5 nm pairs, and, finally, a 0.1 μm p-GaN contact layer. The doping concentrations are 5×10^{18} cm^{-3} for p-type and 1×10^{18} cm^{-3} for n-type. The LD area is 1 μm × 400 μm, and the reflectivity of the two end facets is 50% each.

5. Results and discussions

5.1 Quantum well number effective laser diodes performance

Figure 2 shows the threshold current, output power, slope efficiency, and DQE of MQW LD as a function of the QW number. Best performance is shown by LD with four QW. This is attributed to a small electron leakage current, uniform distribution of electron carriers, and enhanced optical confinement at this number of QW.

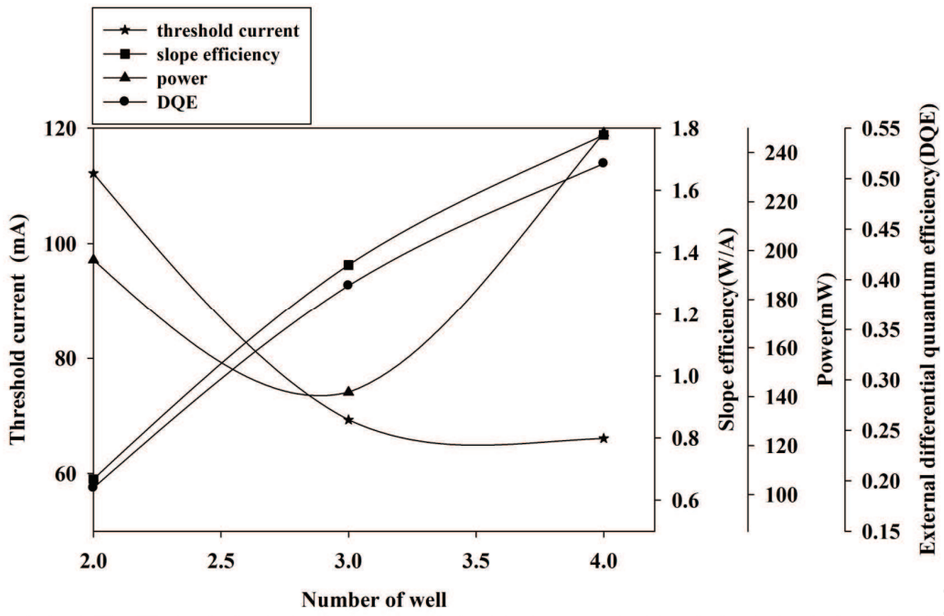

Fig. 2. The output power, threshold current, slope efficiency and DQE of $Al_{0.08}In_{0.08}Ga_{0.84}N/Al_{0.1}In_{0.01}Ga_{0.89}N$ LDs as a function of the quantum wells number.

5.2 Cavity length dependence of the threshold current and DQE

The effect of the cavity length of FQW LD on the threshold current and DQE is shown in Figure 3. The threshold current, representing by the slope efficiency increases with the decreasing in cavity length due to the increasing in mirror losses [Eq. (8)]. The external differential quantum efficiency DQE increases with increasing cavity length. The best values for threshold current, output power, slope efficiency, and DQE of four QW LD at a cavity length of 400 μm are 31.7 mA, 267 mW, 1.91 W/A, and 0.55, respectively. Longer cavity length is not recommended due to induced scattering phenomenon within the gain material of the laser structure.

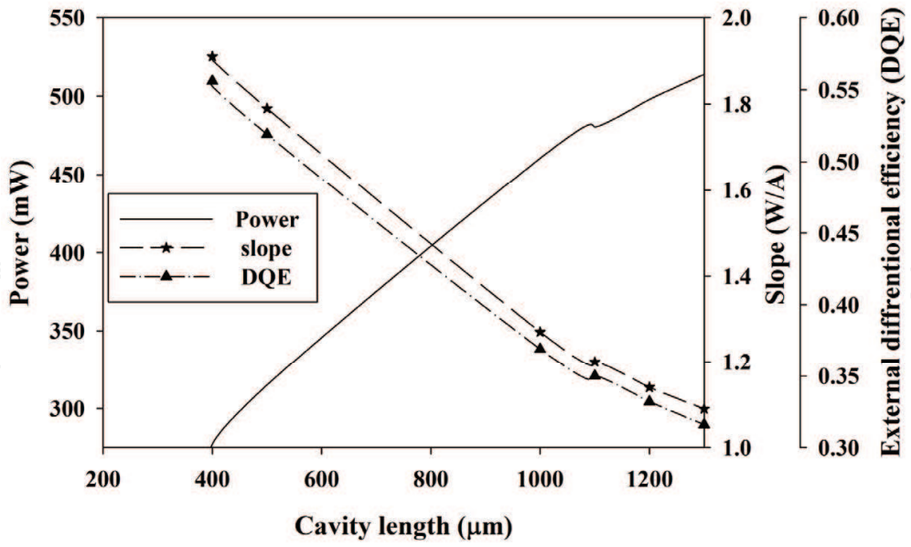

Fig. 3. The output power, slope efficiency and DQE of ($Al_{0.08}In_{0.08}Ga_{0.84}N/Al_{0.1}In_{0.01}Ga_{0.89}N$) LDs as a function of cavity length.

5.3 LD internal quantum efficiency ηi and internal loss

The internal quantum efficiency η_i and internal loss α_i values of the $Al_{0.08}In_{0.08}Ga_{0.84}N/Al_{0.1}In_{0.01}Ga_{0.89}N$ for four QW LD are calculated using Eq. (11). Figure 4 shows that at L = 0, η_i and α_i are equal to 71.4 % and 6.92 cm^{-1}, respectively, which show that good optimization of the geometrical condition of L = 400 μm considered when designing the LD.

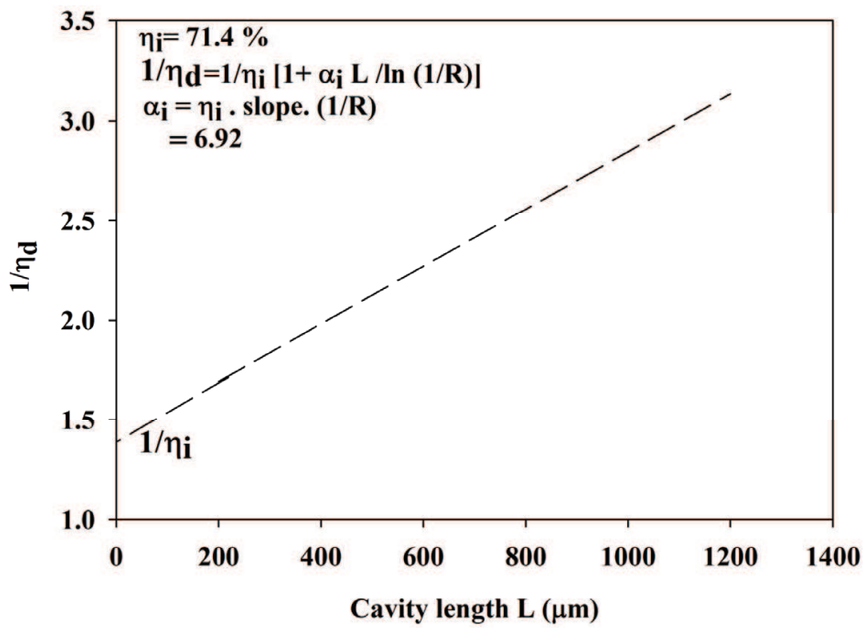

Fig. 4. The inverse DQE of ($Al_{0.08}In_{0.08}Ga_{0.84}N/Al_{0.1}In_{0.01}Ga_{0.89}N$) LDs as a function of cavity length.

5.4 Transparency threshold current density Jth

Figure 5 shows the threshold current density as a function of inverse cavity length. Hence, the intercept of the linear fit line with the vertical axis represented the transparency threshold current value J_0. The four QW LD have a J_0 value of 9.7 KA/cm², which is an acceptable value if compared with ternary LD due to the lattice match between $Al_{0.08}In_{0.08}Ga_{0.84}N$ well and $Al_{0.1}In_{0.01}Ga_{0.89}N$ barriers.

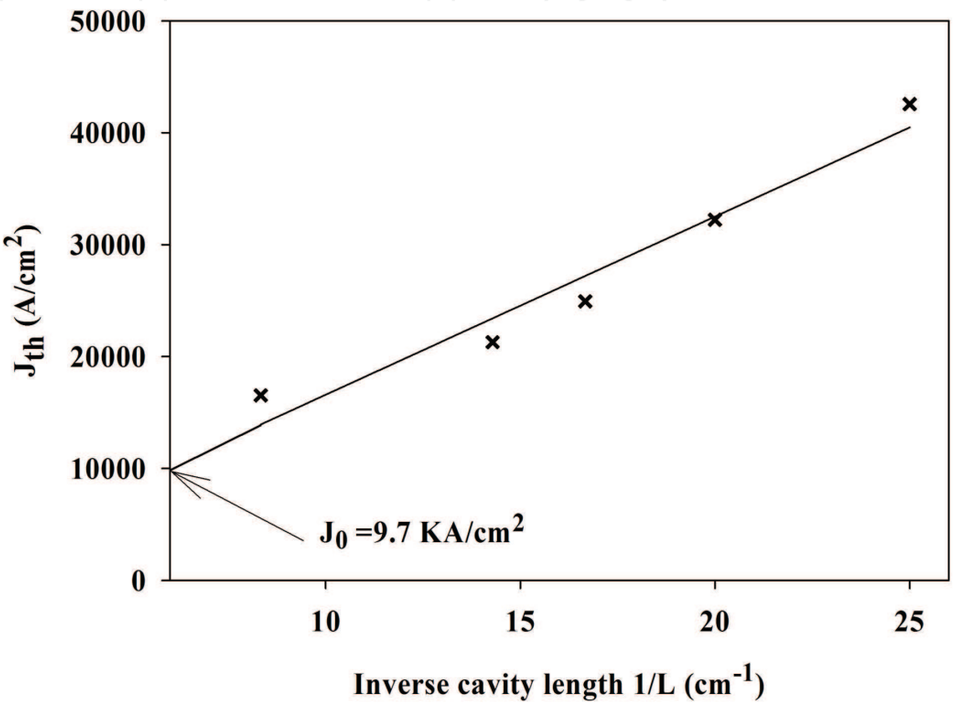

Fig. 5. Transparency threshold current density J_0 value of MQW LD.

5.5 Characteristic temperature T_0

Figure 6 shows the characteristic temperature T_0 value of four QW LD by plotting the natural logarithm of the threshold current density ln (J_{th}) on the y-axis with temperatures on the x-axis. The inverse of the slope of this plot (the linear fit to this set of data point) is the characteristic temperature T_0, which is found to be 97.5 K.

This value is somewhat lower than the characteristic temperature of ternary InGaN LD. This can be explained by the non-uniform distribution of the hole carrier density between wells due to the poor hole mobility in the InGaN layer. However, quaternary AlInGaN alloy is indeed the promising material to be used for well, barrier, and blocking layer. For a more non-uniform hole density distribution between the wells, the hole carriers require additional thermal energy to overcome the barrier potential between the wells. When the temperature increases, the hole density at the n-side of the QW increases due to the thermally enhanced hole transport from the p-side to the n-side of the QW. As a result, the gain at the n-side increases, and the thermal contribution of the hole carrier overflow is reduced with decreasing mirror loss. The characteristic temperature thus increases.

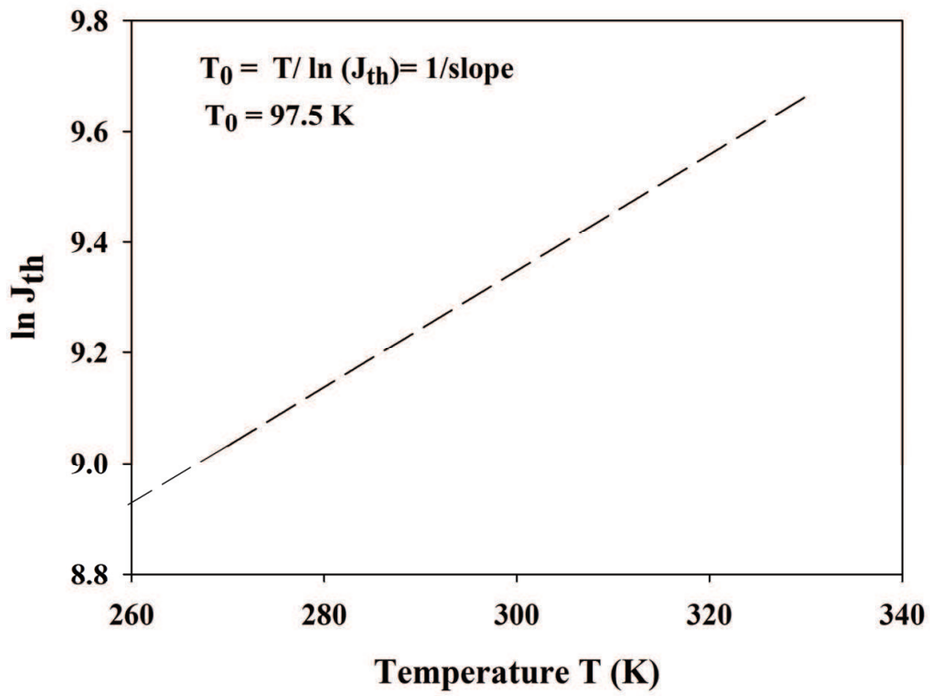

Fig. 6. The characteristic temperature T_0 value of four QWs LD.

6. Summary

The cavity length of quaternary $Al_{0.08}In_{0.08}Ga_{0.84}N/Al_{0.1}In_{0.01}Ga_{0.89}N$ MQW LD plays an important role in LD performance. The influence of cavity length on the threshold current, slope efficiency, characteristic temperature, and transparency threshold current density is studied. A higher characteristic temperature and suitable transparency current density can be obtained by decreasing the mirror loss. High characteristic temperature of 97 K, high output power of 267 mW at room temperature, and low threshold current density of 31.7 mA were achieved by applying a cavity length of 400 μm.

7. Acknowledgments

The authors would like to thank the University Science Malaysia (USM) for the financial support under the 1001/PFIZIK/843088 grant to conduct this research.

8. References

[1] Haase, M. A., Qiu, J., DePuydt, J. M., & Cheng, H. (1991). Blue-green diode lasers. *Appl. Phys. Lett.* Vol. 59, No.11, 1272-1274.

[2] Jeon, H., Ding J., Patterson W., Nurmikko A. V., Xie W., Grillo D. C., Kobayashi M., & Gunshor R. L. (1991). Blue-green injection laser diodes in (Zn,Cd)Se/ZnSe quantum wells. *Appl. Phys. Lett.* Vol. 59, No. 27, 3619-3621.

[3] Nakamura, S., Senoh M., & Mukai T. L8. (1993). p-GaN/N-InGaN/N-GaN double heterostructure blue-light-emitting diodes. Jpn. J. Appl. Phys. 32 (lA–B),

[4] Nakamura, S., Senoh, M., Nagahama, S., Iwasa, N., Yamada, T., Matsushita, T., Kiyoku, H., & Sugimoto, Y. (1996). InGaN-based multi-quantum-well-structure laser diodes. Jpn. J. Appl. Phys. 35 (IB), L74.

[5] Akasaki, I., Sola, S., Sakai, H., Tanaka, T. Koike, M., & Amano H. (1996). Shortest wavelength semiconductor laser diode, Electron. Lett. 32 (12), 1105.

[6] Nagahama S., Yanamoto T., Sano M., & Mukai T. (2001). Characteristics of Ultraviolet Laser Diodes Composed of Quaternary AlInGaN. *Jpn. J. Appl. Phys.* Vol. 40, L 788–L 791.

[7] Nagahama, S., Yanamoto T., Sano M., & Mukai T. (2001). Ultraviolet GaN single quantum well laser diodes. *Jpn. J. Appl. Phys.* Vol. 40, L785-L787

[8] Masui S., Matsuyama Y., Yanamoto T., Kozaki T., Nagahama S., & Mukai T. (2003). 365 nm ultraviolet laser diodes composed of quaternary AlInGaN alloy. *Jpn. J. Appl. Phys.* Vol. 42, L1318–L1320.

[9] Michael K., David W. T., Mark T., Naoko M., & Noble M. J. (2003). Ultraviolet InAlGaN multiple-quantum-well laser diodes. *Phys. Stat. Sol.* Vol. (a) 200, No. 1, 118–121.

[10] Nagahama, S., Iwasa N., Senoh M., Matsushita T., Sugimoto Y., Kiyoku H., Kozaki T., Sano M., Matsumura H., Umemoto H., Chocho K., & Mukai T. (2000). High-power and long lifetime InGaN multi-quantum-well laser diodes grown on low-dislocation-density GaN substrates. *Jpn. J. Appl. Phys.* Vol. 39, L647-L650.

[11] He Y., Song Y., Nurmikko A. V., Su J., Gherasimova M., Cui G., & Han J. (2004). Optically pumped ultraviolet AlGaInN quantum well laser at 340 nm wavelength. *Appl. Phys. Lett.* Vol. 84, No. 4, 463–465.

[12] Seoung–Hwan P., Hwa–Min K. & Doyeol A. (2005). Optical Gain in GaN Quantum Well Lasers with Quaternary AlInGaN Barriers. *Jpn. J. Appl. Phys.* Vol. 44, 7460–7463.

[13] Michael K., Zhihong Y., Mark T., Cliff K., Oliver S.t, Peter K., Noble M. J., Sandra S., & Leo J. S. (2007). Ultraviolet semiconductor laser diodes on bulk AlN. *J. Appl. Phys.*, Vol.101, 123103–123107

[14] Thahab S. M., Abu Hassan H., & Hassan Z. (2009). InGaN/GaN laser diode characterization and quantum well number effect. *CHINESE OPTICS LETTERS* Vol. 7, No. 3, 226-230.

[15] Iqbal Z., Egawa T., Jimbo T., & Umeno M., *IEEE PHOTONIC TECHNOLOGY LETTER.*

[16] Integrated System Engineering (ISE TCAD) AG, Switzerland, *http://www.synopsys.com*

[17] Thahab S. M., Abu Hassan H., & Hassan Z. (2007). Performance and optical, characteristic of InGaN MQWs laser diodes. *Opt. Exp.*, Vol.15, No.5, 2380-2390.

[18] Ghazai A. J., Thahab S. M., Abu Hassan H., & Hassan Z. (2011). A study of the operating parameters and barrier thickness of $Al_{0.08}In_{0.08}Ga_{0.84}N/Al_xIn_yGa_{1-x-y}N$ double quantum well laser diodes, *SCIENCE CHINA TECHNOLOGICAL SCIENCES*, Vol. 54, No. 1, 47–51.

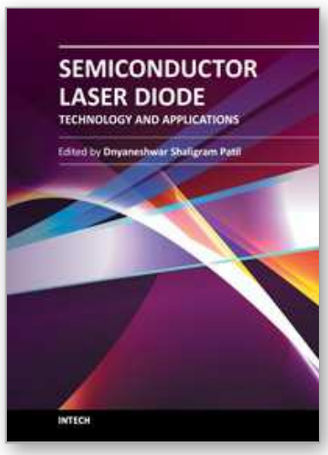

Semiconductor Laser Diode Technology and Applications

Edited by Dr. Dnyaneshwar Shaligram Patil

ISBN 978-953-51-0549-7
Hard cover, 376 pages
Publisher InTech
Published online 25, April, 2012
Published in print edition April, 2012

This book represents a unique collection of the latest developments in the rapidly developing world of semiconductor laser diode technology and applications. An international group of distinguished contributors have covered particular aspects and the book includes optimization of semiconductor laser diode parameters for fascinating applications. This collection of chapters will be of considerable interest to engineers, scientists, technologists and physicists working in research and development in the field of semiconductor laser diode, as well as to young researchers who are at the beginning of their career.

How to reference

In order to correctly reference this scholarly work, feel free to copy and paste the following:

Alaa J. Ghazai, H. Abu Hassan and Z. Hassan (2012). Effect of Cavity Length and Operating Parameters on the Optical Performance of Al0.08In0.08Ga0.84N/ Al0.1In0.01Ga0.89N MQW Laser Diodes, Semiconductor Laser Diode Technology and Applications, Dr. Dnyaneshwar Shaligram Patil (Ed.), ISBN: 978-953-51-0549-7, InTech, Available from: http://www.intechopen.com/books/semiconductor-laser-diode-technology-and-applications/effect-of-cavity-length-and-operating-parameters-on-the-optical-performance-of-al0-08in0-08ga0-84n-a

INTECH
open science | open minds

InTech Europe
University Campus STeP Ri
Slavka Krautzeka 83/A
51000 Rijeka, Croatia
Phone: +385 (51) 770 447
Fax: +385 (51) 686 166
www.intechopen.com

InTech China
Unit 405, Office Block, Hotel Equatorial Shanghai
No.65, Yan An Road (West), Shanghai, 200040, China
中国上海市延安西路65号上海国际贵都大饭店办公楼405单元
Phone: +86-21-62489820
Fax: +86-21-62489821

IntechOpen